

Comparison between step strains and slow steady shear in a bubble raft

Michael Twardos and Michael Dennin

Department of Physics and Astronomy, University of California at Irvine, Irvine, California 92697-4575

(Dated: November 14, 2018)

We report on a comparison between stress relaxations after an applied step strain and stress relaxations during slow, continuous strain in a bubble raft. A bubble raft serves as a model two-dimensional foam and consists of a single layer of bubbles on a water surface. For both step strains and continuous strain, one observes periods of stress increase and decrease. Our focus is on the distribution of stress decreases, or stress drops. The work is motivated by apparent disagreements between quasistatic simulations of flowing foam and simulations of continuous strain for foam. Quasistatic simulations have reported larger average stress drops than the continuous strain case. Also, there is evidence in quasistatic simulations for a general divergence of the average size of the stress drops that only appears to occur in steady strain near special values of the foam density. In this work, applied step strains are used as an approximation to quasistatic simulations. We find general agreement in the dependence of the average stress drop on rate of strain, but we do not observe evidence for a divergence of the average stress drop.

PACS numbers: 83.80.Iz,83.60.La,83.50.-v

I. INTRODUCTION

An open question in the flow of foam is the correspondence between “true” quasistatic flow and constant rate of strain in the limit that the rate of strain approaches zero. (For reviews of foam and the flow behavior of foam, see for instance Refs. [1, 2, 3]). Experiments and simulations of model foams under constant rate of strain clearly exhibit limiting behavior in which the properties of the system become independent of the rate of strain for small enough rates of strain [4, 5, 6, 7, 8, 9]. This has been referred to as the *quasistatic limit*. However, simulations have also been carried out in which a small step strain is applied to the system and the system is allowed to relax to a local energy minimum [10, 11, 12]. Such simulations are referred to as *quasistatic*. Surprisingly, results from quasistatic simulations and results from the quasistatic limit disagree with regard to certain aspects of the flow. This raises important questions not only for the flow behavior of foam, but also for a wide class of complex fluid materials, including granular systems, suspensions, colloids, and emulsions.

Understanding the quasistatic limit of complex fluids, along with glasses and supercooled liquids, is important in the context of the proposal that jamming provides a general theoretical framework in which to study these systems [13, 14, 15]. Jamming refers to the topological crowding of constituent particles, arresting their further exploration of phase space. The jamming phase diagram proposes the existence of a “jammed” state of matter as a function of temperature, stress and inverse density [13, 15]. For materials with a yield stress, such as foam, there is an important connection between the jamming transition and the quasistatic limit. One definition of the yield stress is the value of stress below which a material behaves like an elastic solid and above which it exhibits “flow”. A careful treatment of the yield stress distinguishes between the transition to plastic deformation and

plastic flow. But, for the purposes of this paper, one can treat the yield stress as the point at which the material “unjams”. For materials with a yield stress that are subjected to a constant rate of strain in the quasistatic limit, the average stress is essentially the yield stress. Therefore, these systems exist in a state that is very close to the jamming transition. So, understanding the behavior of foam, or other materials, in the quasistatic limit is one way of probing the nature of the proposed jamming transition.

An open question for the jamming transition is whether or not it is a “true” phase transition. One feature of such transitions is the existence of divergences that exhibit well-defined scaling behavior. These issues have been explored in some detail for the case of zero stress as a function of density [16]. However, the question of the behavior at non-zero stress is still open. For foam, the issue of divergences and scaling behavior has been explored in some detail, even before the proposal of a jamming transition. This is particularly true for measurements of “avalanches” or stress drops in response to an applied strain. Under applied strain (whether continuous or step-strain), foam initially responds in an elastic fashion. In this regime, the stress increases with strain. For sufficiently large applied strain, foam undergoes irregular periods of stress increase and decrease. Loosely speaking, a stress drop is a period of stress decrease, and stress drops are typically associated with nonlinear particle rearrangements. A long standing question in the study of foam is the nature of the distribution of stress drops and the length scales associated with regions of particle rearrangements.

Stress drops have been studied in a wide range of simulations, including the bubble model [4, 5], the vertex model [17, 18, 19], the q-potts model [20], and a quasistatic model [10, 11]. (It should be noted that for periodic foams in two-dimensions, analytic calculations of the stress under continuous shear have been carried out and

interesting changes in the nature of the stress drops as a function of the fluid content are predicted [21]. However, these results are not directly applicable to the random systems discussed here.) Stress relaxations have been measured directly in experiments utilizing bubble rafts [8, 9] and indirectly in other foam systems [6, 22, 23]. Results for the distribution of stress drops vary, but essentially divide into two categories with respect to the nature of stress drops. For the most part, simulations of a constant rate of strain, even in the quasistatic limit, report a distribution of stress drops that has a well-defined average value [4, 5, 24]. In these simulations, there is no evidence for a diverging length scale as a function of rate of strain. There is some evidence of diverging behavior as a function of density, at both the limit of a completely dry foam [17, 18, 19] and as a foam melts [24]. In contrast, a number of quasistatic simulations [10, 11, 12], as well as recent work that models plastic flow in general [25], suggest that a diverging length scale does exist. Experiments that measure stress directly agree with the constant rate of strain simulations [8, 9]. There have been experiments that only measure bubble rearrangements. These appear to divide along the line of the simulations, with continuous strain experiments showing no evidence of a divergence [6, 22] and quasi-static measurements suggesting the existence of large scale events [23]. These results raise two important questions. Is there a fundamental difference between quasistatic step strains and constant rate of strain? Or, is the difference in results simply a manifestation of differing definitions of stress drops?

This paper compares measurements of stress drops using two different types of applied strain. First, we reproduce earlier results for constant rate of strain experiments in bubble rafts [8, 9]. Second, we study stress drops in response to applied step strains that are well separated by periods of waiting. With these experiments, we are able to compare the impact of various definitions of stress drops on measurements of the average stress drop. Also, we directly compare experimental studies with quasistatic simulations. As will be discussed in more detail, the step strains studied here are probably not true “quasistatic” steps in the same sense as is used in simulations. However, they do share many qualitative features with quasistatic steps, and the results provide some insights into differences between quasistatic step strains and steady rate of strain.

II. EXPERIMENTAL SETUP

Our system is a two dimensional foam system referred to as a bubble raft. The Couette viscometer used to generate applied strain and measure the resultant stress is described in detail in Refs. [9, 26]. The basic setup consists of two concentric “cylinders” that confine the bubbles in an annular region on the surface of water. The outer cylinder is a Teflon barrier composed of 12 segmented pieces. The barrier is able to compress and

expand, so as to adjust the density of the bubble raft. It is also able to rotate to generate either constant rates of strain or well-defined step strains. The inner barrier is suspended on a torsion wire and is free to rotate. By measuring the rotation angle, the stress generated in the bubble raft is measured. The creation and characteristics of the bubble raft are discussed in detail in Ref. [8, 9]. Essentially, nitrogen gas is bubbled through a solution of 80% water, 15% glycerine, and 5% Miracle Bubbles (Imperial Toy Corp.). The needle size and flow rate is adjusted to select the bubble distribution. A random size distribution of bubble radii ranging from 1 mm to 5 mm is used.

In this work, we focus on the nature of stress drops and the response to different types of strains applied. In addition, we consider the importance of the definition of a stress drop. To achieve these tasks, the focus is on step strain measurements. Step strains are generated by rotating the outer barrier at a relatively fast constant angular speed for a relatively short time period. Then, the outer barrier is held fixed for a selected time interval. This measurement is designed to parallel quasistatic simulations of foam in which the system is strained an increment and then energy is minimized. There are two aspects to a “true” quasistatic step that must be considered. First, the step itself should be small enough that it almost always produces a reversible deformation. Therefore, stress drops, associated with plastic deformations, should be rare. We will discuss the degree to which our system captures this feature later. Second, the system is relaxed until a minimum energy is found. In the experiments, we do not have access to direct measurements of the energy. So, we can not determine at what point the energy of the system has achieved a minimum after the application of a step strain. Therefore, in order to facilitate comparison with theory, we systematically increased the waiting time until the results were independent of the waiting time. The expectation is that, at least in some statistical sense, this implies we are usually waiting until the energy is minimized.

There are three main variables of importance that define the step strains. They are the angular speed of the strain increment, Ω , the time for rotation, t_{rot} , and the time allowed for relaxation, t_{rel} . One way to consider step strain measurements is to take the total angular displacement applied in a step and divide it by the time it took to strain it plus the time allowed for relaxation. This will provide an effective rotation rate.

$$\Omega_{eff} = \frac{\Omega t_{rot}}{t_{rot} + t_{rel}} \quad (1)$$

It should be noted that because we are applying rapid, small strains, the bubble motions during the strain are essentially elastic. After the strain is stopped, the bubbles are either stationary or undergo nonlinear rearrangements. Therefore, the conversion of effective rotation rate to a rate of strain is not meaningful. In the case of constant applied rate of strain, the average bubble motions

throughout most of the system are found to be consistent with various continuum models for fluids [27], so a definition of the rate of strain is possible. Therefore, for the purposes of this paper, the constant rate of strain results will also be reported in terms of the angular rotation rate, Ω , of the outer barrier. It is important to note that the rate of strain in the Couette geometry is a monotonic function of Ω [28]. Therefore, comparisons of effective rotation rate and actual rotation rate will provide insight into the connection between the quasistatic limit of constant strain rate and the step strain experiments. For a given effective rotation rate, we can probe different time scales and different dynamics by straining it for longer and longer times while allowing the system to relax by a proportionally increasingly long time. One question that can be considered is how an effective rotation rate compares to the actual rotation rate at that value. Are the stress drop distributions similar? Are the average stress values comparable?

It is important to take note of two distinct regimes of step strains. On one side are steps so small (much smaller than a particle diameter) that they are unlikely to independently induce a stress drop during the strain. The small step strains from a theoretical standpoint are the model experimental method to investigate the long time scale dynamics of infinitely slow strain rates. In theory, such an experimental procedure would allow microstepping strains which would be held by the solid like properties of the complex fluid in some jammed configuration. On the other side is step strains that are large, that namely have reached steady state flow and average stress values by inducing several particle rearrangements. As the focus of this paper is comparison with the quasistatic limit of continuous rates of strain and with quasistatic simulations, we focus on the case of small step strains. In the following experiments, we selected a rotation of 0.01 rad/s for 1 second. This choice was largely fixed by the physical limitations of the apparatus. However, it did correspond to a displacement that is less than a typical bubble diameter throughout the system. These experiments were all performed close to the time of creation of the bubble raft, within the first hour of creation when essentially no bubbles were observed to pop.

III. RESULTS

Figure 1 shows a typical response from a series of small step strains. On the scale of the plot, each step strain corresponds to a sudden increase in the stress. The subsequent relaxation occurs during the waiting period. For the first couple of steps, the system is clearly behaving as an elastic solid, and the stress remains constant after a step strain. Furthermore, up until roughly 250 s, the average stress is increasing linearly with the applied strain. However, above approximately 0.5 dyne/cm, the individual steps begin to exhibit relaxation after the initial stress increase. Finally, the average value of the

stress levels off after sufficient strain at a value of approximately 1 dyne/cm. These last two facts are consistent with observations from continuous rate of strain experiments that suggest a yield stress on the order of 0.8 dyne/cm [9, 27]. Also, the agreement between the average stress for the step strains and the continuous rate of strain suggest that it is reasonable to compare the two types of flow.

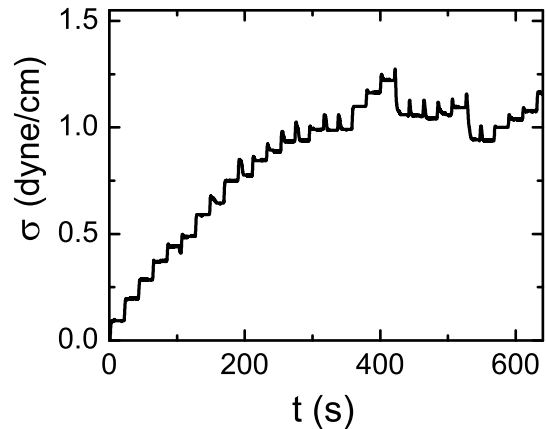


FIG. 1: A plot of the stress versus time for step strain measurements with a step time of 1 second at a rotation rate of 0.1 rad/s and a relaxation time of 20 seconds.

Figure 2 illustrates a close up of multiple relaxation events that illustrate the range of responses to a step strain. The dotted lines mark the end of the step and the onset of a relaxation. Any given relaxation has two possible outcomes. First, the final stress can be greater than the stress *before* the application of the step strain. This is a stress increase. Or, the final stress can be lower than the stress before the application of the step strain. This is one definition of a *stress drop* for the quasistatic case. Independent of the final value of the stress, the relaxation process often occurs through multiple relaxations and plateaus indicative of the complex nature of the stress relaxation. The plateau regions presumably correspond to “quasibasins” during which the energy is still decreasing, but the decrease is releasing essentially no stress, until the system suddenly finds itself rapidly approaching a new value of stress. The fact that multiple plateaus occur complicates the determination of a true stress minimum during relaxation. This is one reason why we used multiple waiting times.

It should be noted that for waiting times greater than 10 s the relaxation plateaus for at least a few seconds before the next step is applied in over 90% of the steps. However, there are rare events where a stress drop is interrupted. The events in Fig. 2 were selected to illustrate one such rare event: the step that occurs at approximately 250 s.

As mentioned, a stress drop is defined as the difference

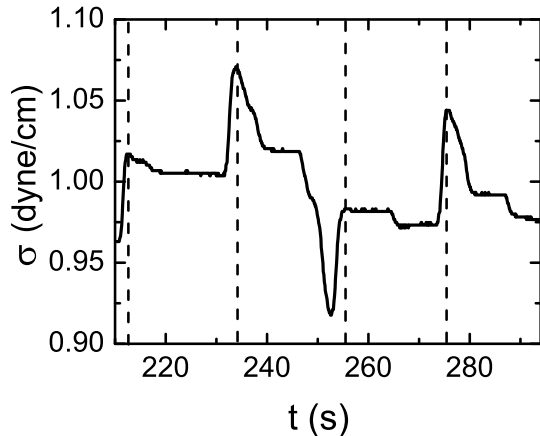


FIG. 2: A closer view of the stress vs. time graph for step strains shown in Fig. 1. The dotted lines mark the end of the step and the onset of a relaxation. The multiple relaxations and plateaus that can be seen following a step strain indicate a complex relaxation time scale.

between one final value of stress just before a new step strain is made (i) and the next one ($i+1$). For purposes of comparing to previous work, we normalize the change in stress by the average stress for the given run ($\langle \sigma \rangle$):

$$\Delta\sigma = (\sigma_i - \sigma_{i+1}) / \langle \sigma \rangle \quad (2)$$

Because we are mainly interested in the stress drops, it should be noted that with this definition a stress *drop* is *positive*.

As described previously, we report results for an applied rotation of 0.01 rad/sec for 1 sec and vary the waiting time. Figure 3 is a plot of the probability distribution for the stress drops for three different waiting times [20 s (\circ), 10 s (\blacksquare), and 1 s (\blacktriangle)]. (Recall, negative stress drops are stress increases.) The important feature to note on the change in stress distribution plots is that the large stress drop tail increases for increasing waiting times up to the time scale of about 20 s. As we will show, for waiting times greater than 20 s, the tail of the stress drop distribution appears to be independent of the waiting time. Two other features of the distribution should be noted. First, the average of the change in stress (including drops and increases) is essentially zero. This is important because it implies that a steady-state has been achieved. The distributions are also asymmetric, with a longer tail for the stress drops. Therefore, the most probable event is a stress increase.

Consideration of Figs. 2 and 3 in some detail provide insight into the question raised earlier concerning the true quasistatic nature of the stress drop. First, Fig. 3 confirms that the most probable event is a stress increase. However, stress increases represent only 57% of the events, not the 90+% of the events one would expect

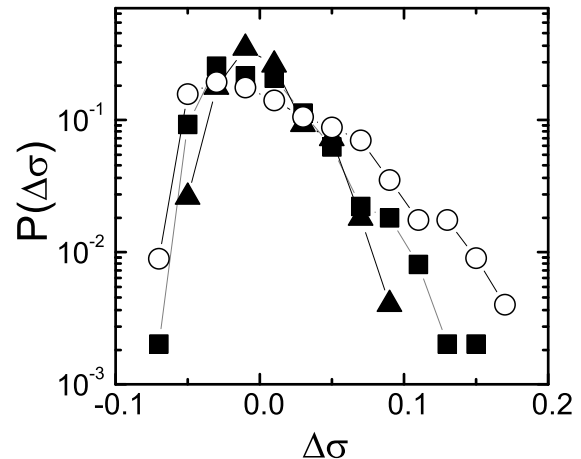


FIG. 3: A distribution of the change in stress defined as the difference between one step strain value and the next. Negative changes in stress correspond to stress increases while positive ones correspond to stress drops. The triangles are a waiting time of 1 second, the squares are 10 seconds and the circles are 20 seconds. As the waiting time is increased across this regime the stress distribution broadens and becomes more asymmetric.

in a true quasistatic situation. Also, essentially all of the stress “increases” involve some relaxation of the stress generated during the applied step strain. This could be due to two effects. First, the applied step occurs at a finite strain rate. Therefore, some fraction of the stress increase is due to viscous effects, and this is expected to relax after the step strain is complete. Such relaxation does not necessarily involve plastic events. The other option is that some irreversible events do occur even during a stress increase. To resolve this issue, detailed measurements of the bubble motions are required. Therefore, it is important to keep in mind that the results reported here are for step strains that only *approximate* a quasistatic step.

Figure 4 is a plot of the probability distribution of only the stress drops and provides a comparison between steady rotation and step strains for one system size. The number of bubbles was 1.05×10^4 . It is important to realize that for continuous rate of strain, the definition of a stress drop is slightly different. In this case, because there is no well defined waiting time, a stress drop is defined as *any* decrease in the stress. This definition was used in our previous measurements [8, 9]. We will discuss the implications of this for the step strain experiments when we discuss the average stress drop size. The solid symbols are for the three different waiting times [1 s (\blacktriangle), 20 s (\blacksquare), and 60 s (\blacksquare)]. The open symbols are for the two different continuous rotation rates [$\Omega = 0.005$ rad/s (\square) and $\Omega = 0.002$ rad/s (\circ)]. For long enough waiting times (> 10 s), the overall shapes of the distributions for con-

tinuous and step strain measurements are similar. There is a clear cutoff at large stress drops, and the probabilities for large stresses are similar. What is not obvious from this plot is the difference for the small stress drops. Closer inspection shows that the continuous strain has significantly more small stress drops. This is not surprising given the two different operational definitions. For the step strain case, the entire relaxation is used, even if it is composed of multiple small steps. The degree to which the small stress drops dominate the continuous rate of strain is best illustrated by considering the average stress drop.

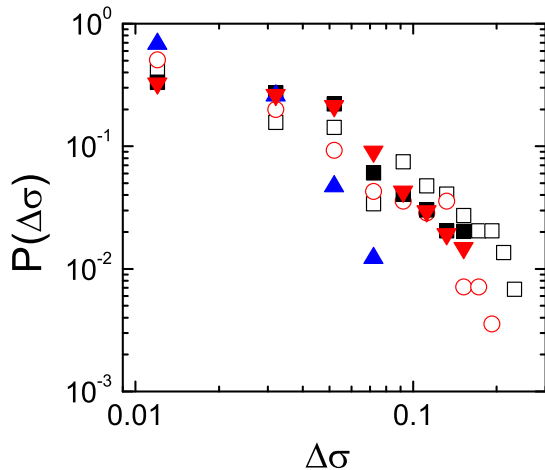


FIG. 4: Probability distribution for only the stress drops for both a series of step strains (closed symbols) and for continuous strain (open symbols). For long enough waiting times (≥ 10 s) the overall shape of the distribution between the two types of flows are similar. The three waiting times for the step strain experiments are 1 s (▲), 20 s (■), and 60 s (■). The two continuous rotation rates are $\Omega = 0.005$ rad/s (□) and $\Omega = 0.002$ rad/s (○). The results highlight the similarities of the step strain and continuous strain distributions for large stress drops.

Figure 5 shows the average stress drop as a function of effective rotation rate for step strains (■) and actual rotation rate for the continuous rate of strain (▲) measurements. Here the dominance of the small stress drops is apparent. For the continuous strain case, we have reproduced the results reported in Ref. [9] that the average stress drop decreases with decreasing rotation rate. For the step strain case, we observe the behavior reported for simulations in Ref. [25] that the average stress drop increases with decreasing rate of strain and reaches a well defined plateau.

To understand better the impact of the definition of the stress drop, we can plot two other quantities. First, for the step strain experiments, we can use the same definition as was used for the continuous rate of strain experiments, where any period of stress decrease is taken as a stress drop. This results in an increase in the number

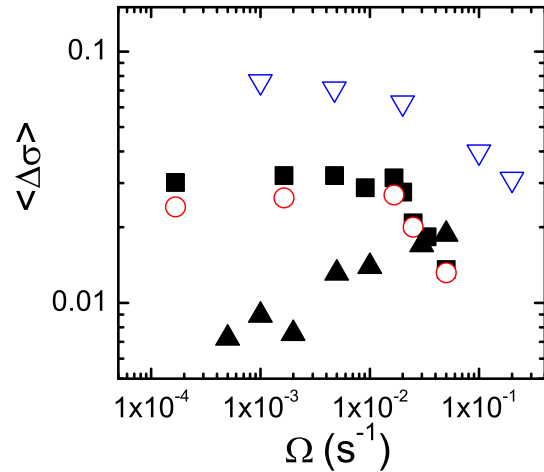


FIG. 5: Plot of the average stress drop as a function of Ω_{eff} for the step strain experiments (■) and as a function of Ω for the continuous strain experiments (▲). Also shown are the results for the step strain experiments with an alternative definition of a stress drop that counts each individual decrease during an entire relaxation event (○), and the alternative definition of stress drops for continuous strain, as discussed in the text (▽). The results highlight the differences between the two types of strain for the average stress drop measurements, as well as the impact of different definitions of a stress drop.

of small stress drops. The results for the average stress drop in this case are given by the open circles in Fig. 5. Here we see that this definition does decrease the average stress drop, but not to the degree that is observed in the continuous rate of strain case.

We also analyze the stress drops in the continuous rate of strain case by the method described in Ref. [25]. In this case, a stress drop is defined by taking an appropriate time interval, τ , and computing $\sigma(t) - \sigma(t + \tau)$. The time interval τ has to be sufficiently large so as not to artificially break up a “typical” stress drop. This is achieved by measuring the average stress drop with increasing values of τ until the measurement is independent of τ . The average stress drop is then defined as $\langle \Delta\sigma \rangle = \langle \sigma(t) - \sigma(t + \tau) \rangle / \langle \sigma \rangle$. Two examples of the dependence of $\langle \Delta\sigma \rangle$ as a function of τ are illustrated in Fig. 6 for two rotation rates. A number of features of the behavior are interesting. First, the value of τ at which $\langle \Delta\sigma \rangle$ becomes independent of τ is an indication of the typical time over which an event occurs. One can see that this is of the order of 10 s in both cases. Second, the time appears to scale with rotation rate (or strain rate), suggesting that the events are best characterized by a typical strain interval.

The results for $\langle \Delta\sigma \rangle$ as measured by computing $\sigma(t) - \sigma(t + \tau)$ are plotted in Fig. 5 (▽), as well. Here we again recover the behavior reported in Ref. [25] that

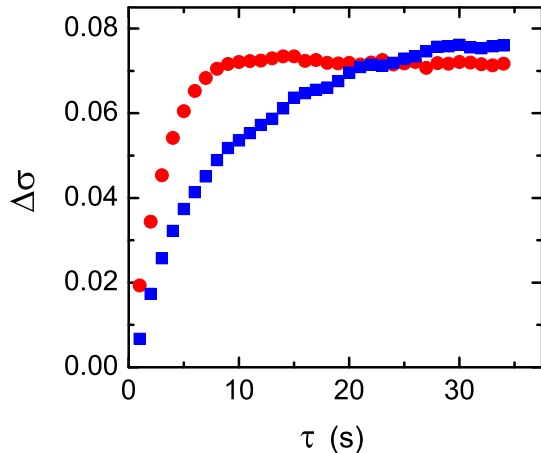


FIG. 6: Plot of $\langle \sigma(t) - \sigma(t + \tau) \rangle$ versus τ for two different rotation rates. The circles are $\Omega = 0.005$ rad/s, and the squares are $\Omega = 0.001$ rad/s. In both cases, the curves plateau for τ on the order of 10 s, with the exact value of the plateau proportional to the rotation rate.

the average stress drop increases with decreasing rate of strain. This result is not too surprising because this alternative definition deemphasizes small stress drops that occur on short time scales. Also, this definition of the average stress drop is related to the variance of the stress as a function of time. The variance was reported in Ref. [9], and behavior similar to that reported in Ref. [25] was observed.

Finally, we considered the system size dependence of the average stress drop. This is illustrated in Fig. 7 for four different system sizes. The system sizes are given using two different measures: the average number of bubbles in the radial direction and the total number of bubbles. Also, we show data for two different effective rotation rates. The triangles correspond to data with a waiting time of 2 s and the squares correspond to data with a waiting time of 60 s. In all cases, there is no evidence of any system size dependence.

IV. DISCUSSION

In this study, we report on measurements of stress relaxations in response to small step strain increments followed by a fixed waiting time. These results are compared with similar measurements under the application of a constant rate of strain. The results show interesting connections between step strain measurements and the constant rate of strain data.

First, the qualitative features of the two measurements are similar. The distribution of stress changes is asymmetric, with a tail for large stress drops. There is a well defined average stress drop for all cases of interest; how-

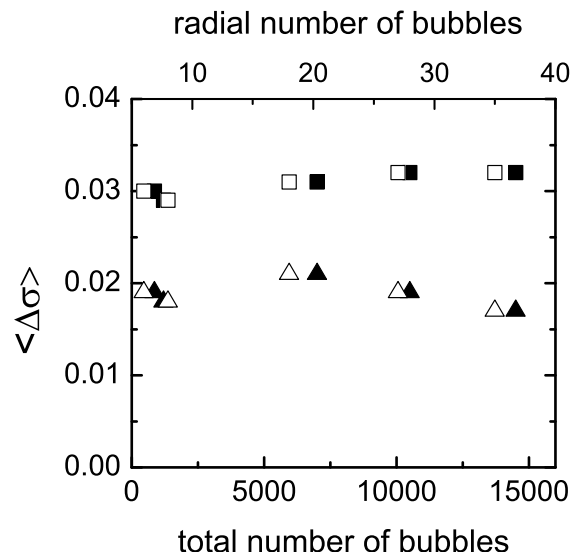


FIG. 7: Plotted here is the system size dependence of the average stress drop for two different waiting times. The squares are for a waiting time of 60 s, and the triangles are for a waiting time of 2 s. The open symbols correspond to the top axis, which gives the average number of bubbles in the radial direction. The closed symbols are relative to the bottom axis. In all cases, no observable system size dependence was measured.

ever, it depends on the definition of stress drop. For continuous rotation, the simplest definition of stress drop results in a decrease in average stress drop with rotation rate. In contrast, a definition that attempts to capture the concept of an “event” rather than an individual stress drop results in a measured increase in the average stress drop with rotation rate. This reflects the occurrence of small stress drops during a single “stress release” event.

Another consistent feature of all of the measurements is the evidence for a “typical” time scale for a stress release event. First, the step-strain measurements suggest a time scale on the order of 10 s based on when these measurements become independent of the waiting time. The measurements from continuous rotation that are based on $\sigma(t) - \sigma(t + \tau)$ also suggest a fundamental time scale on the order of 10 s. In this case, it is important to note that the strain rate does enter as well into determining the average time for an event. Finally, the previous measurements gave a strain rate of 0.07 s^{-1} for the crossover to a quasistatic limit under continuous strain [9]. This also suggests a fundamental time scale on the order of 10 s for this system. The obvious question to ask is the source of the time scale. This is easily done within the context of the bubble model [4]. In the bubble model, bubbles are treated as overlapping circles that interact through a spring force and viscous dissipation. There is only a single time scale in this model, $\tau \approx b/\sigma$, where b sets the scale of the viscous dissipation and σ is the surface

tension of the bubbles. Future work will involve varying these quantities to further explore this fundamental time scale.

When comparing the continuous rotation and the step strain experiments, it is interesting to note that similar definitions of stress drops (considering individual decreases in stress between periods of increase or plateaus) do not give similar results. As expected, for the step-strain case, this definition results in a reduction of the measure average stress drop compared to considering simply the entire stress relaxation during a step. In contrast, during continuous rotation, this definition results in an even lower measured average stress drop. This is evidence for dynamical differences between the slow, steady strain rates and the step strains that is probably consistent with the results for the measurement of τ when determining $\langle \sigma(t) - \sigma(t + \tau) \rangle$. Even though τ is of the same order of magnitude as other measured time scales, it is clearly dependent on Ω . As the rotation rate is decreased, the time for a single event increases. This presumably increases the opportunity for small stress drops to occur, reducing the measured average stress drop. In contrast, for step strains, waiting longer does not impact the number of small stress drops that occur, it simply increases the length of the final plateau on average. These results suggest that there is a fundamental difference between a step strain and continuous rotation that needs to be accounted for when comparing simulations and experiments. Future studies of the bubble motions will help elucidate the differences between these two types of applied strain.

Finally, we have considered the possibility that the average stress drop is system size dependent. Scaling with system size has been observed in at least two different simulations of plastic-type flow [12, 25]. For the range of system sizes studied here, we observed no dependence on the system size for either long or short waiting times

in the step-strain experiments. This was also the case for the average stress drops measured previously [9]. In making this comparison, it should be noted that the step strains are not truly quasistatic and the geometry of the experiments is different from the simulations in a potentially significant fashion. Despite the clear differences between the continuous strain and the step strain, it may be that the step strain is still not a sufficiently good approximation of quasistatic to capture the length scale divergence.

In regards to the geometry, the simulation uses a square box that is scaled up in size. For our system, the system size was varied by increasing the radial dimension of the system. Though this does lead to a corresponding increase in the azimuthal direction, the azimuthal direction remains periodic for all system sizes, and the radial direction has fixed boundaries. This has the effect that bubble rearrangements in the azimuthal direction are free to be as large as they want. As we are measuring the azimuthal stress, this may be the source of the size independence of the average stress drop. This is an aspect of the experiments that can be explored in the simulations. Also, experiments are planned to directly measure the spatial distribution of bubbles involved in the stress releases. Initial measurements of individual bubble motions were inconclusive with regard to the issue of the existence of system-wide events [29], so further work is required.

Acknowledgments

This work was supported by the Department of Energy grant DE-FG02-03ED46071. The authors thank Craig Maloney, Andrew Kraynik, and Lydéric Bocquet for useful discussions.

-
- [1] A. M. Kraynik, *Ann. Rev. Fluid Mech.* **20**, 325 (1988).
 - [2] J. Stavans, *Rep. Prog. Phys.* **56**, 733 (1993).
 - [3] D. Weaire and S. Hutzler, *The Physics of Foams* (Clarendon Press, Oxford, 1999).
 - [4] D. J. Durian, *Phys. Rev. Lett.* **75**, 4780 (1995).
 - [5] D. J. Durian, *Phys. Rev. E* **55**, 1739 (1997).
 - [6] A. D. Gopal and D. J. Durian, *Phys. Rev. Lett.* **75**, 2610 (1995).
 - [7] G. Debrégeas, H. Tabuteau, and J. M. di Meglio, *Phys. Rev. Lett.* **87**, 178305 (2001).
 - [8] J. Lauridsen, M. Twardos, and M. Dennin, *Phys. Rev. Lett.* **89**, 098303 (2002).
 - [9] E. Pratt and M. Dennin, *Phys. Rev. E* **67**, 051402 (2003).
 - [10] D. Weaire, F. Bolton, T. Herdtle, and H. Aref, *Phil. Mag. Lett.* **66**, 293 (1992).
 - [11] S. Hutzler, D. Weaire, and F. Bolton, *Phil. Mag. B* **71**, 277 (1995).
 - [12] C. Maloney and A. Lemaitre, *Phys. Rev. Lett.* **93**, 016001 (2004).
 - [13] A. J. Liu and S. R. Nagel, *Nature* **396**, 21 (1998).
 - [14] A. J. Liu and S. R. Nagel, eds., *Jamming and Rheology* (Taylor and Francis Group, 2001).
 - [15] V. Trappe, V. Prasad, L. Cipelletti, P. N. Segre, and D. A. Weitz, *Nature* **411**, 772 (2001).
 - [16] C. S. O'Hern, L. E. Silbert, A. J. Liu, and S. R. Nagel, *Phys. Rev. E* **68**, 011306 (2003).
 - [17] K. Kawasaki, T. Nagai, and K. Nakashima, *Phil. Mag. B* **60**, 399 (1989).
 - [18] K. Kawasaki, T. Okuzono, T. Kawakatsu, and T. Nagai, in *Proc. Int. Workshop of Physics of Pattern Formation*, edited by S. Kai (Singapore: World Scientific, 1992).
 - [19] T. Okuzono and K. Kawasaki, *Phys. Rev. E* **51**, 1246 (1995).
 - [20] Y. Jiang, P. J. Swart, A. Saxena, M. Asipauskas, and J. A. Glazier, *Phys. Rev. E* **59**, 5819 (1999).
 - [21] D. A. Reinelt and A. M. Kraynik, *J. Fluid Mech.* **215**, 431 (1990).
 - [22] M. Dennin and C. M. Knobler, *Phys. Rev. Lett.* **78**, 2485

- (1997).
- [23] A. A. Kader and J. C. Earnshaw, *Phys. Rev. Lett.* **82**, 2610 (1999).
 - [24] S. Tewari, D. Schiemann, D. J. Durian, C. M. Knobler, S. A. Langer, and A. J. Liu, *Phys. Rev. E* **60**, 4385 (1999).
 - [25] G. Picard, A. Ajdari, F. Lequeux, and L. Bocquet, *cond-mat/0409452* (2004).
 - [26] R. S. Ghaskadvi and M. Dennin, *Rev. Sci. Instr.* **69**, 3568 (1998).
 - [27] J. Lauridsen, G. Chanan, and M. Dennin, *Phys. Rev. Lett.* **93**, 018303 (2004).
 - [28] R. B. Bird, R. C. Armstrong, and O. Hassuage, *Dynamics of Polymer Liquids* (Wiley, New York, 1977).
 - [29] M. Dennin, *Phys. Rev. E* **70**, 041406 (2004).